International Journal of GEOMATE, Aug., 2024 Vol.27, Issue 120, pp.9-16
ISSN: 2186-2982 (P), 2186-2990 (O), Japan, DOI: https://doi.org/10.21660/2024.120.4117
Geotechnique, Construction Materials and Environment

SEISMOTECTONIC ANALYSIS OF M_W 7.6 2023 SOUTH MOLUCCA INTERMEDIATE-DEPTH EARTHQUAKE

Djati Kuncoro[1,2], *Yusran Asnawi[3], Yehezkiel Halauwet[1], Andrean Simanjuntak[1], Adi Susilo[4]

[1]Indonesia Agency for Meteorology Climatology and Geophysics, Jakarta, Indonesia
[2]Department of Environmental, Graduate Program and School, Universitas Brawijaya, Indonesia
[3]Department of Information and Tecnology Education, Universitas Islam Negri Ar-Raniry, Indonesia
[4]Department of Physics, Faculty of Mathematics and Natural Sciences, Universitas Brawijaya, Indonesia

*Corresponding Author, Received: 04 Aug. 2023, Revised: 25 April 2024, Accepted: 10 May 2024

ABSTRACT: On January 10, 2023, a significant earthquake with M_w 7.6 occurred in the southern part of Molucca, Indonesia, and generated widespread ground shaking around IV-VI MMI, followed by building damages and early tsunami warning. The hypocenter was located deeper than the common slab contour, which may indicate another blind tectonic system called intraslab. Joint analysis was applied by correlating the waveform inversion with hypocenter relocation to identify the current seismic activities. The main objective of the finding results is to configure the seismotectonic system that has generated several intermediate-depth earthquakes in the southern part of Molucca. Therefore, a total of 1711 earthquakes were obtained from the 2019 - 2022 catalog which were recorded by 72 stations associated with 9125 P-phase and 4217 S-phase. As many as 90% (1530) of the total earthquakes were successfully relocated, while 10% (170) were not relocated because they did not meet the predetermined criteria. Furthermore, the mainshock was resolved with thrusting fault with NW – SE orientation, steeply dipping to the SW direction and a moment magnitude estimation M_w of 7.6 ± 0.03 at depth 35.50 ± 2 km. The focal parameters include two nodal planes, i.e., first nodal plane with strike 319°, dip 15.5° and rake 101°, and second nodal plane with strike 127°, dip 74.8° and rake 86.8°. The results show successfully the existence of the hidden intraslab beneath the collision between the Australian plate and the Eurasian plate, which can provide new insight and also contribute to the recent tectonic system in East Indonesia

Keywords: Earthquake, Intraslab, Hypocenter relocation, Moment tensor, Molucca, Subduction, Tectonic

1. INTRODUCTION

On January 10, 2023, a significant earthquake with M_w 7.6 occurred in the northernmost part of Molucca, Indonesia. Previously, there were two largest earthquakes that generated significant ground shaking on June 24, 2019 with M_w 7.1 and on December 29, 2021 with M_w 7.2. The Indonesia Meteorological Geophysical and Climatology Agency (BMKG) reported that the M_w 7.6 earthquake caused significant ground shaking around IV–VI MMI followed by a tsunami early warning. Several geophysical agencies (USGS, GFZ, GCMT, and IPGP) proposed the earthquake mechanism to be a thrusting mechanism, striking in the NW-SE direction perpendicular to the trench line. The thrusting mechanism suggests a possible faulting from the subduction process. However, the location and depth of the earthquake occurred deeper than the common slab contour, that may indicate another possible tectonic system.

Tectonically, the southern region of Indonesia is categorized as an earthquake-prone area due to its location in the active tectonic system. Several major earthquakes have occurred due to the collision process of the Australian plate subducting towards and beneath the Eurasian plate with 2 – 3 cm/yr at a dipping angle of 40–60° [1,2]. Seismically, the southern part of Molucca is located on the active tectonic system (see Fig. 1), and conveniently generates several significant earthquakes, such as Seram with M_w ~8.2/8.5 in 1629, Banda Arc with M_w ~8.4 in 1852, and Banda Sea with M_w 8.5 in 1938 [3,4]. Lastly, two devastating earthquakes occurred in the Flores Sea with M_w 7.8 in 1992, and M_w 7.5 in 2004, followed by significant tsunami run-up and massive damages that impacted the local community in the coastal area [5]. Several major earthquakes have recently occurred with M_w ~7 such as in 2019 with M_w 7.2, in 2021 with M_w 7.2 and, in 2023 with M_w 7.6. The sequence of M_w ~7 in the intermediate depth of 100 – 300 km suggests an active deep tectonic system. On the other hand, the Timor collision in the western part of Banda Arc is categorized as an active seismic zone but locked and could represent a future major earthquake followed by a potential tsunami [6].

Several studies have been conducted to determine the tectonic and seismic activities in the study area, such as the seismic profile in the outer Banda arc between Sumba Island and Savu Island and offshore West and East Timor Island [3,7]. The variation of the tectonic system makes a consistent predominant mode of deformation, and has formed a frontal accretion where recent trough fill, slope sediments, and continental-margin strata from Australia are folded and thrusted above a decollement [8-10]. Several studies aimed to characterize the active deformation along East Indonesia and the entire trough system, which is required for further earthquake and tsunami hazard assessment [4,5,11-13]. However, to our knowledge, there is a lack of seismic studies that have been conducted to configure and explain the current activities of the intermediate-depth earthquakes in the southern part of Molucca, as illustrated in Fig. 1.

In the present study, the analysis focuses on studying the last largest earthquake with M_w 7.6. Hypocenter relocation using a double-difference earthquake location algorithm and statistical analysis was applied to highlight the temporal and earthquake clusters. Moreover, the moment tensor inversion was applied to configure the faulting mechanism. The results successfully determine the characteristics of the intermediate-depth tectonic system that is responsible for the M_w 7.6. Furthermore, the results suggest an essential finding that configures a north dipping slab from the intermediate deep tectonic system in East Indonesia.

2. RESEARCH SIGNIFICANCE

The presence of the intermediate deep tectonic system may provide a tectonic characteristic of the responsible system. The results can be used to assess future major earthquakes with similar faulting in the study area. An understanding of the various tectonic systems can support the mitigation program for the felt earthquake in East Indonesia based on the seismological study.

3. MATERIALS AND METHODS

3.1 Seismic Data and Hypocenter Relocation

In this study, the arrival time is used to relocate the earthquake hypocenter, which is important in configuring a specific cluster. The earthquake criteria were set so that: the number of seismic phases must be 10 with a minimum of 4 S-phases, the hypocenter criteria have a depth range at 0 - 200 km, azimuth gap coverage is < 180°, and the distance between hypocenters with station distribution is 0 – 4°. Two categories of seismic data were used to understand the tectonic process: body-wave seismic arrival times (P and S phases) and the waveform of the mainshock.

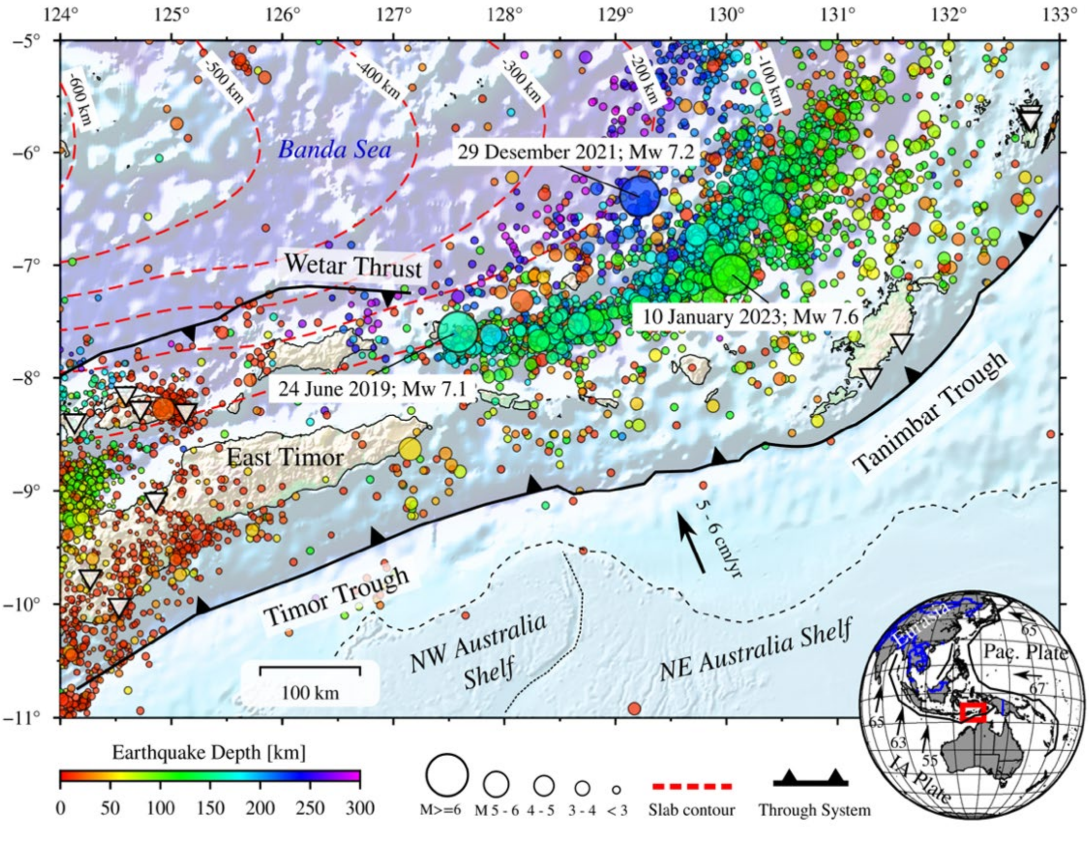

Fig. 1 Map showing the tectonic systems and seismicity in the southern part of Molucca Island. The subduction zone has been formed by the collision between the Australian and Eurasian plate with 5 - 6 cm/year [1,2].

In the last decade, the Meteorology, Climatology, and Geophysics Agency (BMKG, Indonesia) has recorded the seismic arrival time at each permanent seismic station. In this case, the arrival time is used to relocate the earthquake hypocenter, which is required to configure the specific earthquake cluster. The earthquake criteria were specified as follows: the number of seismic phases must be 10 with a minimum of 4 S-phases, the depth range must be 0 - 200 km, the azimuth gap coverage must be 180°, and the distance between hypocenters with seismic station must be below 4°. Based on these criteria, a total of 1750 earthquakes recorded by 48 sensors between 2019 and 2022 were obtained from the catalog (Fig. 2).

The total number of seismic phases compiled for hypocenter displacement is 9125 P-phase and 4217 S-phase. Precise earthquake location is essential to configure the detailed structure obtained from hypocenter relocation. The HypoDD program [14] was used in this case to cluster the hypocenter based on relative relocation. The fundamental algorithm of HypoDD assumes that the distance between two earthquakes is less than the distance to the station, and that the raypath medium is always identical. In the iterative method, HypoDD reduces the residual between the observed and calculated travel time variations. The hypocenter position will be changed after each iteration to minimize the residual between observed and calculated.

3.2 Bayesian Moment Tensor Inversion

For the mainshock, seismic waveform was used to evaluate the earthquake mechanism through Bayesian moment tensor inversion. The waveform data were collected from an open-access seismic network approximately 2000 km distance from the epicenter. Using the Grond probabilistic inversion framework, the inversion strategy was applied to the three rotating components (Z, Radial, and Transversal) [15].
Grond tools has been widely applied to analyze several significant earthquakes in Indonesia [16-19]. To highlight an uncertainty in the nonlinear model, the Grond employs the Bayesian technique with a bootstrap optimization. The distribution of subsequent models significantly updates information based on the tested models, until the improved parameters are equal or smaller and have a converged solution.

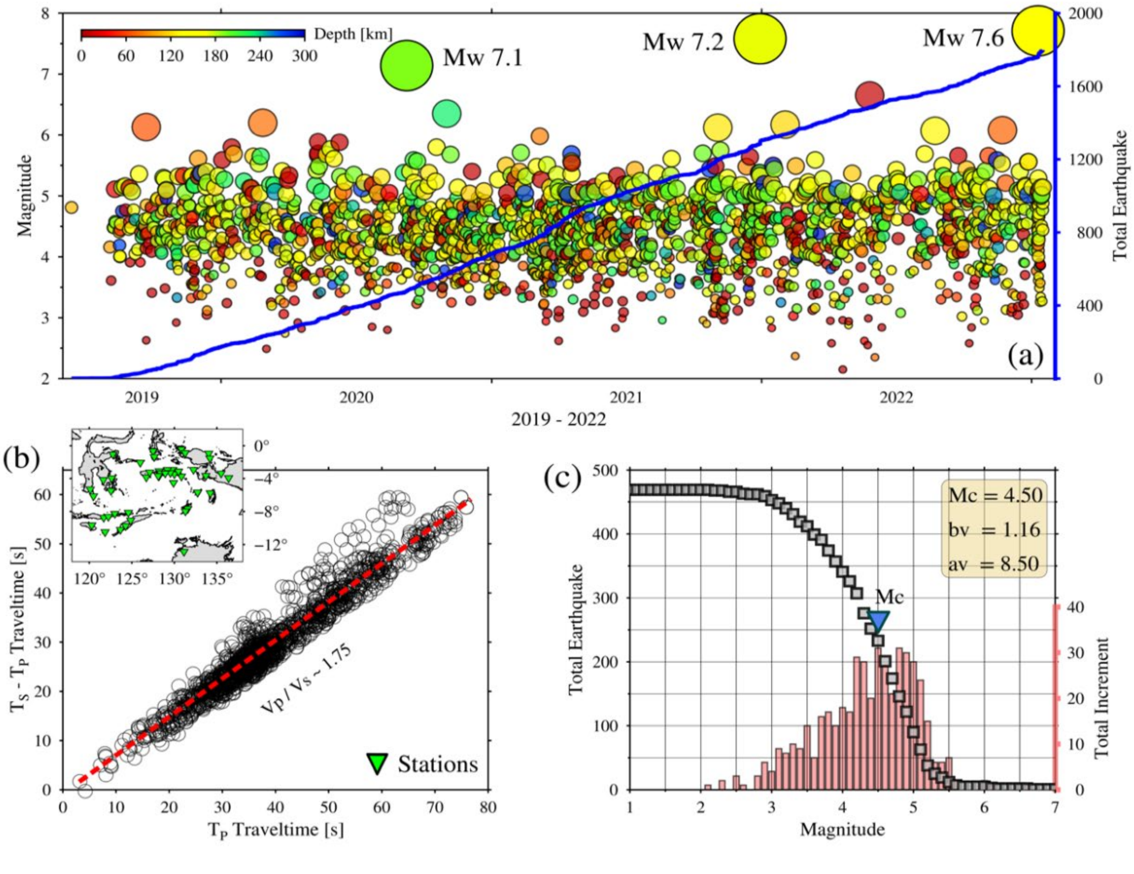

Fig. 2 (a) Temporal graph showing earthquake distribution in the four-year catalogue. (b) The arrival time graph of P and S waves with $V_p/V_s \sim 1.75$. (c) Magnitude histogram gives three statistical parameters M_c 4.5, b_v 1.16, and a_v 8.5 that show the quality of seismic network in the study area.

4. RESULTS AND DISCUSSION

The hypocenter relocation processing used the velocity model from Simanjuntak et al. [20] that is derived from the study of slab gap beneath Toba. The shifting hypocenter location and depth give values with range 10 - 20%. Using the double difference method, the updated hypocenter provides a more precise location and cluster.

The criteria applied for relative relocation were a maximum separation of 30 km, a maximum number of neighbors per event of 50 km, and an 8-phase minimum number of connections required to determine neighbors. As a result, the conjugate gradient for least-squares (CGLS) method was chosen to relocate a large number of earthquakes since it is more efficient. As proposed by Waldhauser [14], the damping parameter was set at 20 to yield a CND parameter between 40 and 80 for the majority of hypocenters found.

The initial data have a high apriori that needs a weighting factor to obtain the relative hypocenter positions in each iteration. Finally, as many as 88% of the total earthquakes were successfully relocated while 103 were not relocated. The relocation results show a significant change in the hypocenter quality.

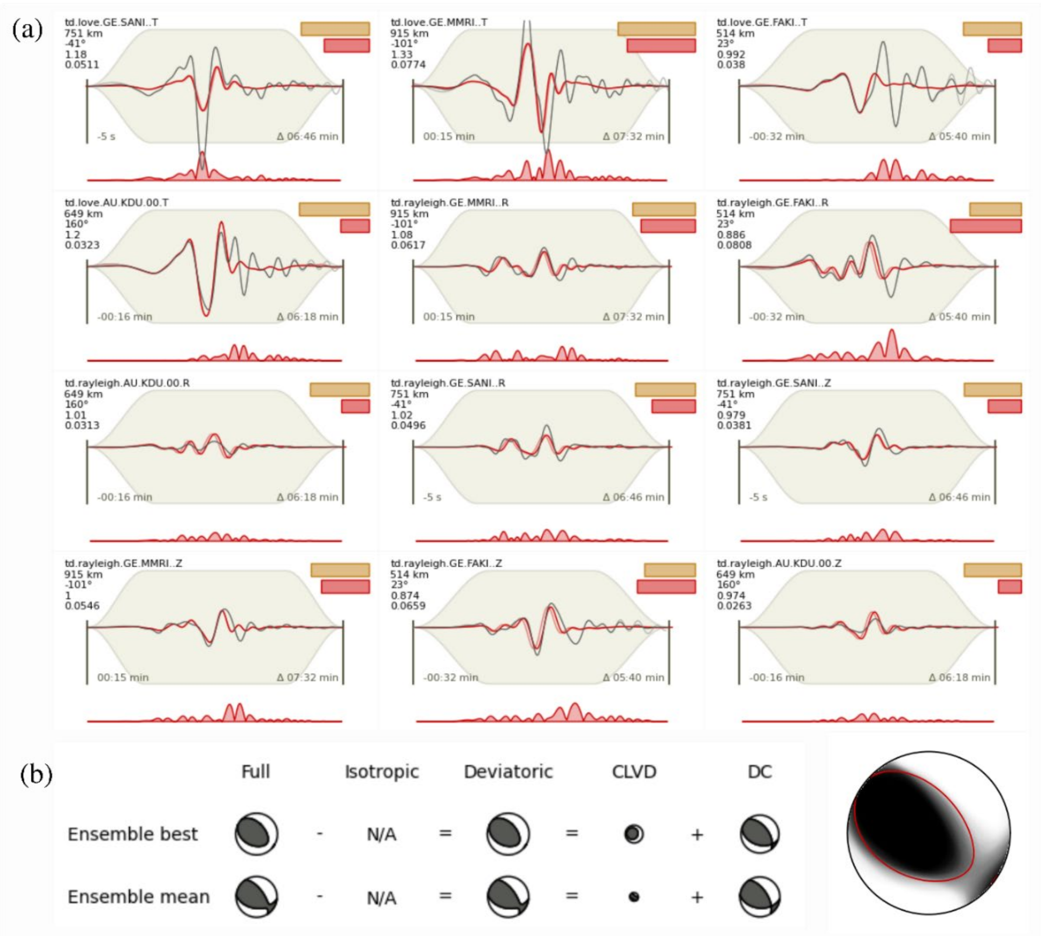

Fig. 3 (a) Results for the M_w 7.6 shows a fitting between the observation (black lines) and synthetic waveforms (red lines). (b) Decomposition percentage results shows the information of the deviatoric component.

For inversion, a Green's functions model from a pre-calculated velocity model with sampling 0.5 Hz was applied with fitted full displacement waveforms for all seismic stations used [25]. The bandpass filter of 0.005 - 0.05 Hz was applied as the common range for major earthquakes with M_w ~7. A total of 3,000 different configurations were given with 50,000 iterations in the optimization process to provide a convergence solution. Finally, the deviatoric component consists of a Compensated Linear Vector Dipole (CLVD) component with 8 ± 1% while the Double Couple (DC) with 92 ± 2% suggests a pure tectonic process responsible for the M_w 7.6.

The focal parameters result (see Fig. 3) contains two nodal planes i.e., first nodal plane with a strike of 319°, a dip of 15.5°, and a rake of 101°, while the second nodal plane was with strike of 127°, dip of 74.8°, and rake of 86.8°. Both nodal planes were calculated by bootstrap analysis with a Bayesian solution that provides a converged solution based on probability density function (PDF). Each PDF graph provides a final solution with low and narrow deviation window that update the focal parameters for the M_w 7.6.

Furthermore, the relationship between focal parameters also shows a converged solution into specific nodal parameters. It can be stated that the velocity model used for the inversion is well-recognized. On the other hand, the focal parameter results are well resolved with a satisfactory uncertainty for two nodal planes (± 2°) and adequate misfit < 0.5 as shown in Fig. 4. The mainshock suggests a rupture propagation towards E-W that was striking parallel with the trench line, steeply dipping to the north direction.

4.1 Seismicity Profile

To see the hypocenter distribution change in the vertical position, three cross sections are given to configure the seismicity in the vertical profile. An oblique line (A-A) was set that crosses the dip angle of the focal mechanism result (second nodal plane) and combines with relocation results (see Fig. 5). The cross section shows three clusters that follow a subduction slab pattern beneath Weber Deep (i.e., deepest point in the Banda Sea off Indonesia), and is responsible for several intermediate earthquakes at depths in the range of 0 - 300 km. The subduction gap is clearly described along the slab with low seismicity at 60 – 120 km depth. The low seismicity can be addressed by the existence of the forearc and front deformation as the accretionary wedge along the trench [4,7]. Therefore, the interface zone has the lowest seismicity with shallow depth.

A cross-section oblique line (A-A) was set that crossed the dip angle of the focal mechanism result and combined with relocation results as shown in Fig. 5. Cross section (A-A) shows the dip angle of the focal mechanism (second nodal plane) with the relocation results (see Fig. 5). The seismic profile from Coudurier-Curveur [3] studied the trench along the trough system and found a lack of seismicity along the trench due to the strength flexure of the collision with Australia. The low seismicity in the interface zone may indicate a locking zone with a possibility of an asperity [20].

The vertical profile of the hypocenter relocation shows there is low seismicity after the forearc-island that started at depth 20 km until reaching 80 km. The hypocenter distribution shows a thrusting system dipping perpendicular to the slab subduction. However, a lack of studies for the intraslab activities in the East Indonesia region may provide an ambiguity for the responsible tectonic system of the recent subduction system from the Australian plate [5].

4.2 Quaternary Subduction and Australian Collision Beneath East Indonesia

The Islands arc in the Banda Sea, from Timor to Seram, have been systematically separated into two regions as the inner and outer arc. The recent arc system that collided with the northern half of

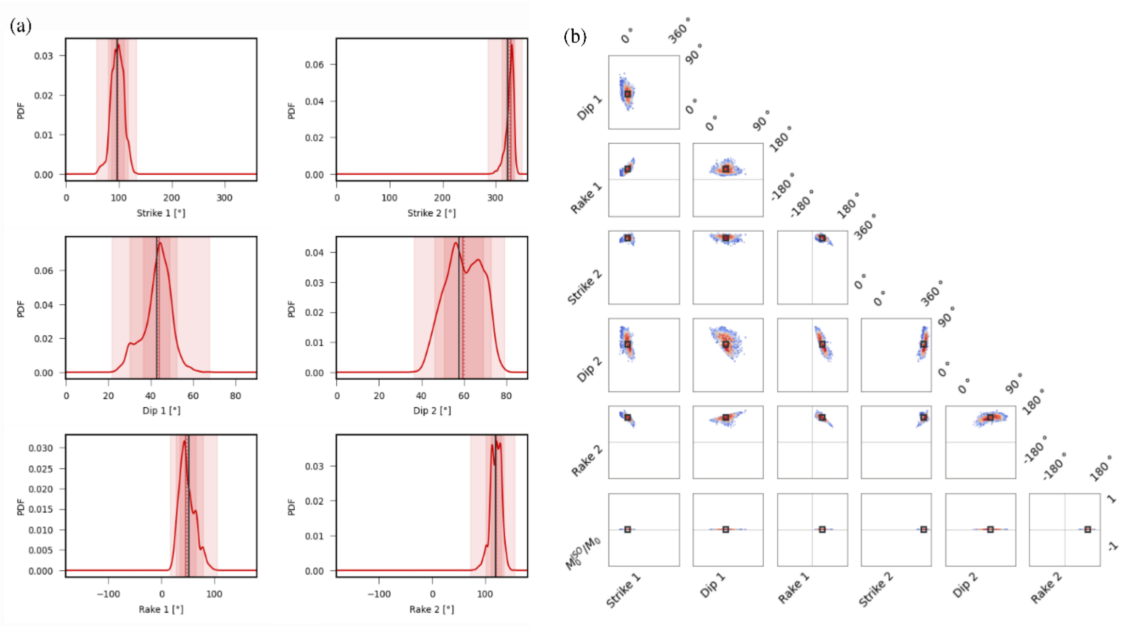

Fig. 4 Probability density function (PDF) graph shows the confidence level for two nodal planes parameters. (b) The joint parameter shows a satisfactory result with a converged solution with a two-parameter relationship.

the Banda embayment is not visible, and the current active volcanic arc stops at Banda at the arc's eastern end [1,3,7]. The geometry of the subducted slab in the mantle under Tanimbar, on the other hand, has led to the commonly held opinion that the system of troughs broadly parallel to the Benioff zone is descriptive equally as the outer arc islands [4,5,7,8,21].

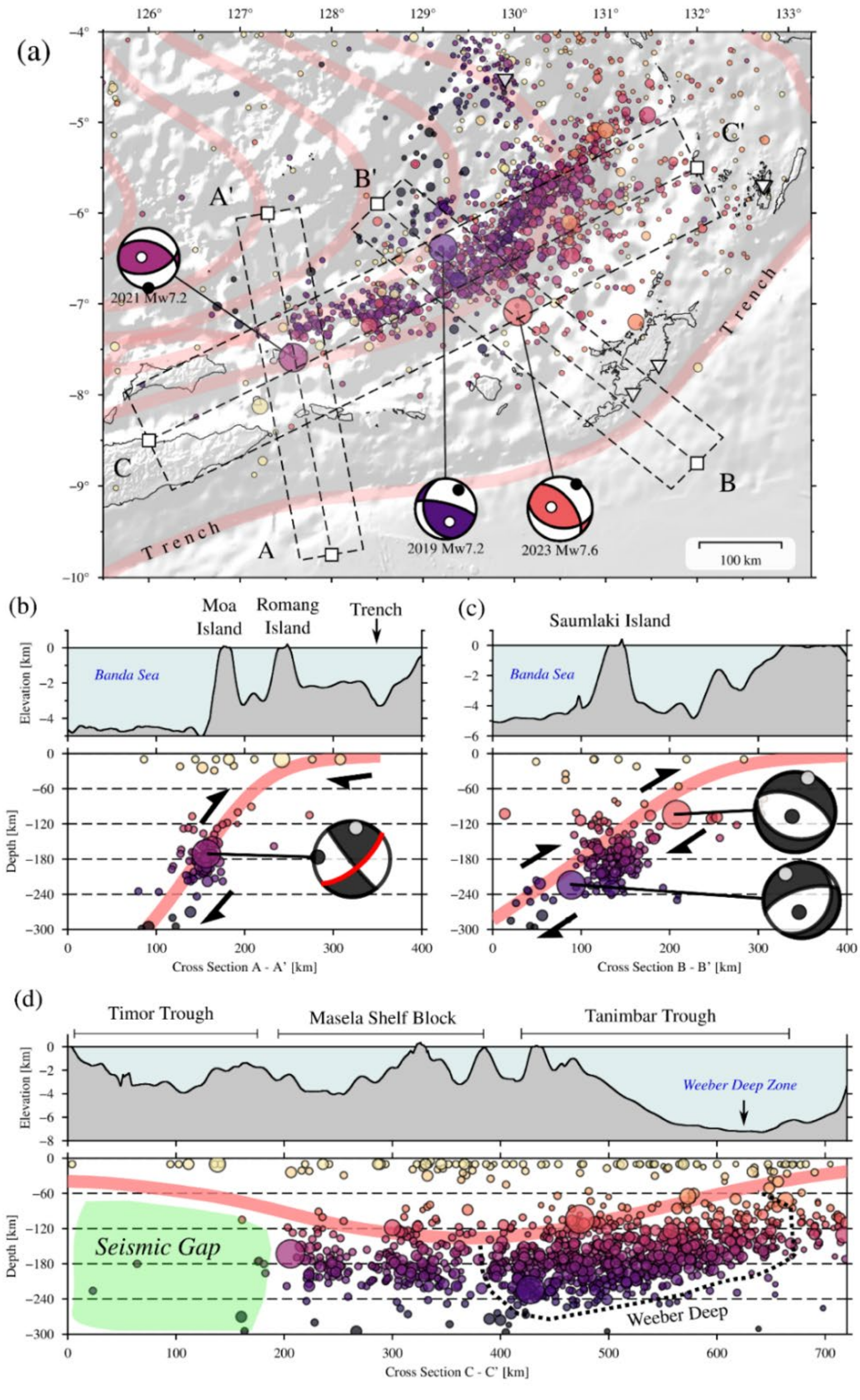

Fig. 5 (a) Seismicity map showing relocated hypocenter with three slices A-A', B-B', C-C'. (b) Slice A-A' and (c) Slice B-B' shows a cluster in the intermediate depth range 100 – 200 km with the focal mechanism. (d) Slice C-C' shows hypocenter clusters and figure the western part (Timor Trough/0 has a possible seismic gap.

The troughs are frequently depicted as a continuous feature, except for the location of the presumed subduction zone, particularly at the eastern end of the arc. There is a trace of a subduction zone from the Tanimbar Trough to the Seram Trough [8,21]. The Seram Trough has been defined as far west as Buru.

Furthermore, a relationship between the spatial and temporal seismicity around the trough system is difficult to estimate based on bathymetric and seismic reflection profiles. However, the present study provides a novel result that shows the activity of late subduction as the responsible system for the M_w 7.6. The results of current seismicity can be used to support disaster mitigation in the near future [22-27]. Nevertheless, a further investigation into the backthrust must be conducted to provide a detailed understanding, especially for the recent tectonic structure.

5. CONCLUSIONS

A joint analysis has been successfully applied by correlating the moment tensor inversion with hypocenter relocation to identify the responsible system that generated an earthquake in the Tanimbar Trough System. 90% of the total earthquakes (1,530 events) were successfully relocated with a thrusting fault that was striking in the NW – SE orientation and M_w of 7.6 ± 0.03 at a depth of 114.50 ± 2 km. The focal parameters include two nodal planes, i.e., first nodal plane with strike 319°, dip 15.5°, and rake 101° while the second nodal plane has strike 127°, dip 74.8°, and rake 86.8°. The results successfully show the existence of the late subduction beneath the southern part of Molucca as the responsible system for the M_w 7.6. The results suggest an essential finding that features a north dipping slab from the intermediate deep tectonic system in the East Indonesia region.

6. REFERENCES

[1] Spakman W., and Hall R., Surface Deformation and Slab–mantle Interaction During Banda Arc Subduction Rollback. Nature Geoscience, Vol. 3, Issue 8, 2010, pp. 562-566.

[2] Rahmadani S., Meilano I., Susilo S., Sarsito D. A., Abidin H. Z., and Supendi P., Geodetic Observation of Strain Accumulation in The Banda Arc Region. Geomatics, Natural Hazards and Risk, Vol. 13, Issue 1, 2022, pp. 2579-2596.

[3] Coudurier-Curveur A., Singh S. C., and Deighton, I., Timor Collision Front Segmentation Reveals Potential for Great Earthquakes in the Western Outer Banda Arc, Eastern Indonesia. Frontiers in Earth Science, Vol. 9, Article 640928, 2021, pp. 1-14.

[4] Okal E. A., and Reymond D., The Mechanism of Great Banda Sea Earthquake of 1 February 1938: Applying The Method of Preliminary Determination of Focal Mechanism to a Historical Event. Earth and Planetary Science Letters, Vol. 216, Issue 1-2, 2003, pp. 1-15.

[5] Cummins P. R., Pranantyo I. R., Pownall J. M., Griffin J. D., Meilano I., and Zhao S., Earthquakes and Tsunamis Caused by Low-Angle Normal Faulting in The Banda Sea, Indonesia. Nature Geoscience, Vol. 13, Issue 4, 2020, pp. 312-318.

[6] Hamzah L., Puspito N. T., and Imamura F., Tsunami catalog and zones in Indonesia. Journal of Natural Disaster Science, Vol. 22, Issue 1, 2000, pp. 25-43.

[7] Kaneko Y., Maruyama S., Kadarusman A., Ota T., Ishikawa M., Tsujimori T., and Okamoto K., On-going Orogeny in the outer-arc of the Timor–Tanimbar region, eastern Indonesia. Gondwana Research, Vol. 11, Issue 1-2, 2007, pp. 218-233.

[8] Audley-Charles M. G., Ocean Trench Blocked and Obliterated by Banda Forearc Collision with Australian Proximal Continental Slope. Tectonophysics, Vol. 389, Issue 1-2, 2004, pp. 65-79.

[9] Brown D., Ryan P. D., Harris R., The Nature of The Banda Arc–continent Collision in The Timor Region. Arc-continent collision, 2011, pp.163-211.

[10] Duffy B., Quigley M., Harris R., and Ring U., Arc-parallel Extrusion of he Timor sector of the Banda Arc-continent Collision. Tectonics, Vol. 32, Issue 3, 2013, pp. 641-660.

[11] Simanjuntak A. V., and Ansari K., Seismicity Clustering of Sequence Phenomena in the Active Tectonic System of Backthrust Lombok Preceding the Sequence 2018 Earthquakes. Arabian Journal of Geosciences, Vol. 15, Issue 23, 2022, 1730.

[12] Pasari S., Simanjuntak A. V., Mehta A., and Sharma Y., The Current State of Earthquake Potential on Java Island, Indonesia. Pure and Applied Geophysics, Vol. 178, Issue 8, 2021, pp. 2789-2806.

[13] Pasari S., Simanjuntak A. V., and Sharma Y., Nowcasting Earthquakes in Sulawesi Island, Indonesia. Geoscience Letters, Vol. 8, Issue 1, 2021, pp. 1-13.

[14] Waldhauser F., hypoDD—A Program to Compute Double-Difference Hypocenter Locations (HypoDD Version 1.0-03/2001). US Geol. Surv. Open File Rep., Open file report 01-113, 2001, pp. 1-25.

[15] Heimann S., Isken M., Kühn D., Sudhaus H., Steinberg A., Vasyura-Bathke H., Daout S.,

Cesca S., and Dahm T. Grond – A Probabilistic Earthquake Source Inversion Framework, GFZ Data Services, V.1.0, 2018, pp.1.
[16] Muksin U., Arifullah A., Simanjuntak A. V., Asra N., Muzli M., Wei S., and Okubo M., Secondary Fault System in Northern Sumatra, Evidenced by Recent Seismicity and Geomorphic Structure. Journal of Asian Earth Sciences, Vol. 245, 2023, pp. 105557.
[17] Simanjuntak A.V.H., and Ansari K., Spatial Time Cluster Analysis and Earthquake Mechanism for Unknown Active Fault (Kalatoa fault) in the Flores Sea. Earth Science Informatics Vol. 7, Issue 1, 2023, pp. 131-145.
[18] Supendi P., Winder T., Rawlinson N., Bacon, C. A., Palgunadi K. H., Simanjuntak A. V., and Jatnika J., A Conjugate Fault Revealed by the Destructive Mw 5.6 (November 21, 2022) Cianjur Earthquake, West Java, Indonesia. Journal of Asian Earth Sciences, Vol. 257, 2023, pp. 105830.
[19] Simanjuntak A.V.H., Palgunadi K. H., Supendi P., Daryon D., Prakoso T. A., Muksin U., New Insight on the Active Fault System in the Halmahera Volcanic Arc, Indonesia, Derived from the 2022 Tobelo Earthquakes. Seismological Research Letters. Vol. 94, Issue 6, 2023, pp. 2586-2594.
[20] Zhan Z., Mechanisms and Implications of Deep Earthquakes. Annual Review of Earth and Planetary Sciences, Vol. 48, 2020, pp. 147-174.
[21] Brown D., Ryan P. D., and Harris R. The Nature of the Banda Arc–continent Collision in the Timor Region. Arc-continent collision, 2011, pp. 163-211.
[22] Muksin U., Riana E., Rudiyanto A., Bauer K., Simanjuntak A. V. H., and Weber M., Neural Network-based Classification of Rock Properties and Seismic Vulnerability. Global Journal of Environmental Science and Management, Vol. 9, Issue 1, 2023, pp. 15-30.
[23] Simanjuntak A. V. H., Muksin U., Arifullah A., Lythgoe K., Asnawi Y., Sinambela, M., and Wei S., Environmental Vulnerability Characteristics in an Active Swarm Region. Global Journal of Environmental Science and Management, Vol. 9, Issue 2, 2023, pp. 211-226.
[24] Asnawi Y., Simanjuntak A., Muksin U., Rizal S., Syukri M., Maisura M., and Rahmati, R., Analysis of Microtremor H/V Spectral Ratio and Public Perception for Disaster Mitigation. International Journal of GEOMATE, Vol. 23, Issue 97, 2022, pp. 123-130.
[25] Simanjuntak A., Muksin U., Asnawi Y., Rizal S., and Wei S., Recent Seismicity and Slab Gap Beneath Toba Caldera (Sumatra) Revealed Using Hypocenter Relocation Methodology. International Journal of GEOMATE, Vol. 23, Issue 99, 2022, pp. 82-89.
[26] Asnawi, Y., Simanjuntak, A., Muksin, U., Okubo, M., Putri, S.I., Rizal, S., and Syukri, M., Soil classification in a seismically active environment based on shear wave velocity and HVSR data. Global Journal Environmental Science Management, Vol. 8, Issue 3, 2022, pp. 297-314.
[27] Simanjuntak, A.V.H., and Ansari, K., Multivariate Hypocenter Clustering and Source Mechanism of 2017 Mw 6.2 and 2019 Mw 6.5 in the South Seram Subduction System. Geotech Geol Eng. Vol. 42, Issue 4, 2024, pp. 1-14.